A SHALLOW WATER MODEL FOR COMPUTING TSUNAMI ALONG THE WEST COAST OF PENINSULAR MALAYSIA AND THAILAND USING BOUNDARY-FITTED CURVILINEAR GRIDS

Md. Fazlul Karim[a], G D Roy[b], Ahmad Izani M Ismail[a], Mohammed Ashaque Meah[a]

mdfazlulk@yahoo.com ; gaurangadebroy@gmail.com; izani@cs.usm.my; mamsust@yahoo.com

[a] *School of Mathematical Sciences*, *Universiti Sains Malaysia*, 11800 *Pulau Pinang*, *Malaysia*
[b] Department of Mathematics, Shahjalal University of Science & Technology, Sylhet, Bangladesh

ABSTRACT

The west coast of Peninsular Malaysia and Thailand is curvilinear in nature and the bending is especially high along the coast of South Thailand. In hydrodynamic models for coastal seas, bays and estuaries, the use of boundary-fitted curvilinear grids not only makes the model grids fit well with the coastline and bathymetry, but also makes the finite difference scheme simple. In this study, a shallow water model is developed using boundary fitted curvilinear mesh. The west coast of Peninsular Malaysia and Thailand and the western open boundary are represented by two curves, which are defined by two functions. The other two boundaries are considered as straight lines along the open sea. Appropriate transformations of independent coordinates are applied so that the curvilinear physical domain transforms to a rectangular domain and the curvilinear grid system transforms to a rectangular system. The depth averaged shallow water equations and the boundary conditions are transformed to the new space domain and these are solved in the rectangular mesh of the transformed space. The model is applied to compute some aspects of the tsunami associated with the 26 December 2004 Indonesian tsunami along the coastal belts of Penang in Malaysia and Phuket in Thailand. The computed results along the coastal belts are in excellent agreement with the observe data available in the USGS website.

Keywords: boundary-fitted curvilinear grid; shallow water model; Indonesian tsunami 2004

Mathematics Subject Classification: 86A05, 86A17

1. INTRODUCTION

The west coasts of Peninsular Malaysia and southern Thailand face an active seismic tsunami source zone (close to Sumatra Island) along the fault line between the Burma and Indian Plates (Fig. 1). Hence, this coastal belt is vulnerable to the effects of seismic sea waves, or tsunamis generated along this fault line. These events are frequent and often cause little or no damage. However, a great earthquake may generate a large tsunami that may cause extensive loss of life and property damage

Figure 1: Model domain including west coast of Thailand, Peninsular Malaysia and source zone west of north Sumatra (Source: Roy et al. 2006)

along these coastal belts. This was demonstrated on 26 December 2004 when a magnitude 9.3 earthquake, which occurred off the west coast of northern Sumatra, Indonesia, generated a most damaging tsunami. Penang Island in Malaysia and Phuket in Thailand were lashed by high tsunami surges and many lives were lost due to the Indonesian tsunami of 2004.

Numerical computation has become a powerful and popular tool to study tsunamis. A number of papers have been published on modeling the Indonesian tsunami of 2004 for the west coast of Southern Thailand and Peninsular Malaysia after the event 26 December 2004 (see, Roy and Ismail. 2005; Roy et at. 2006; Karim et al. 2006). The analysis area is a rectangular region approximately between 2° N to 14° N and 91° E to 101.5° E for all of these studies. The model area includes the source region of the Indonesian tsunami of 2004. These models are based on depth-averaged shallow water equations and were discretized by the finite-difference scheme in Cartesian coordinate system with the shoreline represented by stair-steps. In a stair step model the coastal boundaries are approximated along the nearest finite difference gridlines of the numerical scheme and so the accuracy of a stair step model depends on the grid size. Since in the stair step models of Roy and Ismail.(2005); Roy et at. (2006) and Karim et al. (2006) very fine resolution were not considered, the representation of the coastal boundaries in those models were not very accurate.

The west coasts of Malaysia and Thailand are curvilinear in nature and the bending is high along the coasts of these countries. Moreover, there are some offshore islands including Penang in Peninsular Malaysia and Phuket in Thailand. For model flows in a rectangular domain, it is natural to use Cartesian grids. Most hydrodynamic models of reservoirs, tidal harbors and estuaries rely on finite difference solution of the depth-averaged equations expressed in a Cartesian coordinate frame (Abbot et al., 1973; Falconer, 1980; Kuipers and Vreugdenhil 1973). In practice, a rectangular mesh with fixed grid spacing is placed over the domain of interest, usually resulting in non-alignment of the physical boundaries with the edges of the computational flow domain. This lack of alignment may give rise to major inaccuracies in the solution. For cylindrical or spherical domains, it is natural to use cylindrical or spherical grids. Hence in the presence of a curvilinear coastline, it is natural to use ‘boundary-fitted’ grids, or generalized curvilinear grids to represent the model boundaries accurately.

Boundary-fitted curvilinear grid systems provide an approach, which combines the best aspects of finite-difference discretisation with grid flexibility. The boundary fitted grid technique makes the equations and boundary conditions simple and better represents the complex geometry with a relatively less number of grid points. Thus, it significantly improves the finite difference schemes. However one difficulty in boundary fitted grid system is that the gridline of the numerical scheme are curvilinear and non-orthogonal. In order to apply a regular finite difference scheme the grid system must be rectangular. In a boundary-fitted model, the curvilinear boundaries are transformed into straight ones using appropriate transformations, so that in the transformed space regular finite difference techniques can be used. Boundary-fitted grid techniques for coastal dynamics have been developed for many regions. Johns et al (1981) used partially boundary-fitted curvilinear grids in their transformed coordinate model for the east coast of India to simulate the surge generated by the Andra Cyclone of 1977. Johns et al. (1981) used a transformation to transform the irregular physical domain

into a rectangular Science of domain. Dube et al. (1985) represented the shoreline of Bangladesh by a curvilinear boundary and used the boundary-fitted curvilinear grids and a transformation, similar to Johns et al. (1981). Roy (1999) developed a mathematical technique to incorporate island of special shapes, each of whose boundaries were approximated along the boundary-fitted grid lines. Following Johns et al.(1981), the transformation of a spatial coordinate was applied so that the physical domain transformed to a rectangular one and the shape of each island also become rectangular in the transformed domain. Johnson (1982) employed the elliptic grid generation technique to study the 2-D vertical-averaged riverine circulation where non-orthogonal boundary-fitted curvilinear grids for the physical domain were generated. Spaulding (1984) built a vertically averaged circulation model using boundary-fitted co-ordinates to simulate the M2 tide in the North Sea. Androsov et al. (1997) made a simulation of tide with a 2-D model in boundary fitted curvilinear mesh.

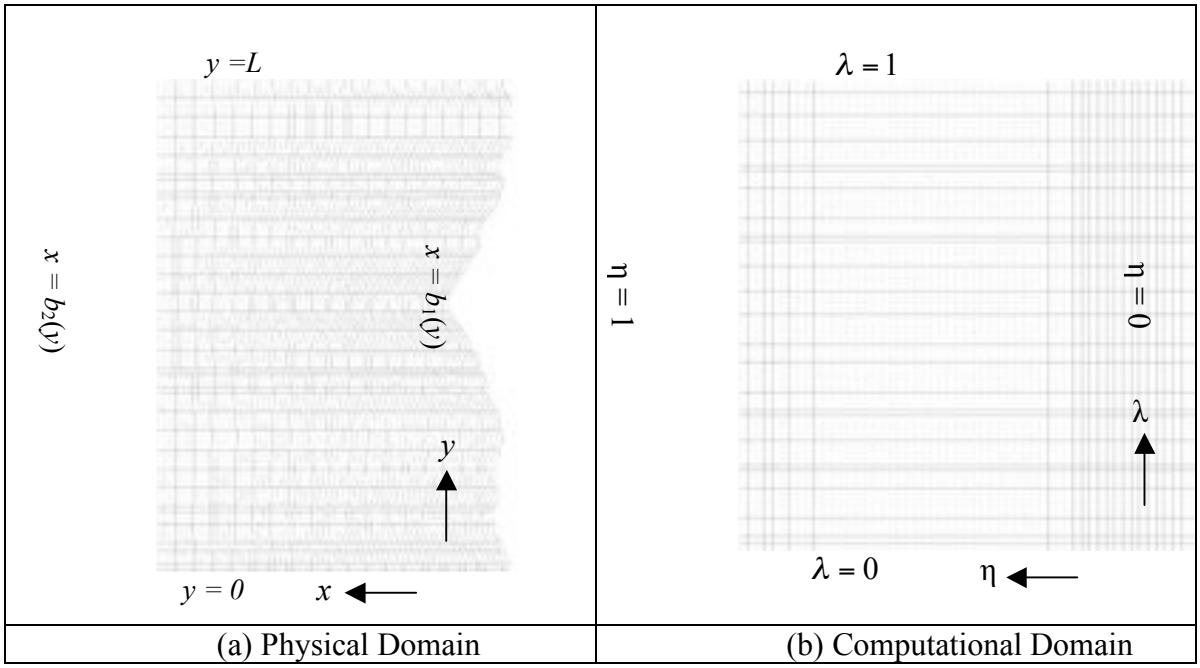

Figure 2: Boundaries and grid system; (a) curvilinear boundaries and the curvilinear grid system, (b) rectangular boundaries and the rectangular grid system

In this paper, a shallow water model is developed using a boundary fitted curvilinear grid system to compute some aspects of the tsunami associated with the Indonesian tsunami of 2004 along the coastal belts of Penang and Phuket. The west coasts of Malaysia and Thailand (curvilinear in nature) and the western open sea boundary were represented by two functions. On the other hand, the north and south open sea boundaries were considered as straight lines. In order to generate a set of non-orthogonal curvilinear grid lines in the model domain and the boundary lines we define two generalized functions. The four boundaries of each island are also represented approximately by these two generalized functions. Two transformations are used so that the physical domain becomes rectangular and the whereabouts of the boundaries of each island are identifiable in the transformed domain. Details of incorporating coastal boundaries and islands are described in section 2.4 and 2.5.

The depth averaged shallow water equations are transformed to the new space domain. These transformed shallow water equations are solved in a rectangular mesh of the transformed grid system in the transformed space using a regular finite difference scheme.

2. GOVERING EQUATIONS AND BOUNDARY CONDITIONS

2.1 *The Original Shallow Water Equations and Boundary Conditions*

The following set of shallow water equations have often been used for modeling tsunami:

$$\frac{\partial \zeta}{\partial t} + \frac{\partial}{\partial x}\left[(\zeta + h)u\right] + \frac{\partial}{\partial y}\left[(\zeta + h)v\right] = 0 \tag{1}$$

$$\frac{\partial u}{\partial t} + u\frac{\partial u}{\partial x} + v\frac{\partial u}{\partial y} - f v = -g\frac{\partial \zeta}{\partial x} - \frac{C_f u\left(u^2 + v^2\right)^{1/2}}{(\zeta + h)} \tag{2}$$

$$\frac{\partial v}{\partial t} + u\frac{\partial v}{\partial x} + v\frac{\partial v}{\partial y} + f u = -g\frac{\partial \zeta}{\partial y} - \frac{C_f v\left(u^2 + v^2\right)^{1/2}}{(\zeta + h)} \tag{3}$$

Here u and v are the x and y components of velocity of sea water respectively, g is gravity, f is Coriolis parameter, ζ is the displacement of the free surface from the equilibrium state, C_f is the bottom friction coefficient, h is ocean depth from the mean sea level.

For numerical treatment it is convenient to express the equations (2) and (3) in flux form by using the equation (1). Equations (1) – (3) may be expressed as

$$\frac{\partial \zeta}{\partial t} + \frac{\partial \tilde{u}}{\partial x} + \frac{\partial \tilde{v}}{\partial y} = 0 \tag{4}$$

$$\frac{\partial \tilde{u}}{\partial t} + \frac{\partial (u\tilde{u})}{\partial x} + \frac{\partial (v\tilde{u})}{\partial y} - f\tilde{v} = -g(\zeta + h)\frac{\partial \zeta}{\partial x} - \frac{C_f \tilde{u}\left(u^2 + v^2\right)^{1/2}}{\zeta + h} \tag{5}$$

$$\frac{\partial \tilde{v}}{\partial t} + \frac{\partial (u\tilde{v})}{\partial x} + \frac{\partial (v\tilde{v})}{\partial y} + f\tilde{u} = -g(\zeta + h)\frac{\partial \zeta}{\partial y} - \frac{C_f \tilde{v}\left(u^2 + v^2\right)^{1/2}}{\zeta + h} \tag{6}$$

where, $(\tilde{u}, \tilde{v}) = (\zeta + h)(u, v)$

2.2 *Boundary Conditions*

For closed (coast) boundaries, the boundary condition is that the normal component of the vertically integrated velocity vanishes and this may be expressed as

$$u\cos\alpha + v\sin\alpha = 0 \qquad \text{for all } t \geq 0 \tag{7}$$

where α denotes the inclination of the outward directed normal to the *x*-axis. It follows that the velocity component *u is* 0 along *y*-directed boundaries and *v is* 0 along *x*-directed boundaries. At the open-sea boundary, the normal component of the velocity cannot vanish and so radiation type of boundary condition is generally used. Following Heaps (1973), the radiation type of boundary condition is

$$u\cos\alpha + v\sin\alpha = -(g/h)^{1/2}\zeta \qquad \text{for all } t \geq 0 \tag{8}$$

Application of a radiation type of boundary condition at the open-sea boundary of a model allows the propagation of energy only outwards from the interior in the form of simple progressive waves.

For $x = b_1(y)$ condition (7) may be simplified as $u + v\tan\alpha = 0$, which implies that $u - v\tan(180-\alpha) = 0$. This can be written as $u - v\dfrac{dx}{dy} = 0$, i.e. $u - v\dfrac{db_1}{dy} = 0$.

Therefore, following Johns et al. (1981), the radiation type of boundary conditions are given by

$$u - v\frac{db_1}{dy} = 0 \qquad \text{at } x = b_1(y) \tag{9}$$

$$u - v\frac{db_2}{dy} = (g/h)^{1/2}\zeta \qquad \text{at } x = b_2(y) \tag{10}$$

$$v + (g/h)^{1/2}\zeta = 0 \qquad \text{at } y = 0 \tag{11}$$

$$v - (g/h)^{1/2}\zeta = 0 \qquad \text{at } y = L \tag{12}$$

2.3 *Boundary-fitted grids*

A system of rectangular Cartesian coordinates is used in which the origin *O*, is within the equilibrium of the sea-surface. *OX* points towards the west, *OY* points towards the north and *OZ* is directed vertically upwards. The displaced position of the sea-surface is given by $z = \zeta(x, y, t)$ and the position of the sea-floor by $z = -h(x, y)$ .The eastern coastal boundary is situated at $x = b_1(y)$ and a western open-sea boundary is at $x = b_2(y)$. The southern and the northern open-sea boundaries are at $y = 0$ and $y = L$ respectively. This configuration is shown in Fig. 2a.

The system of gridlines oriented to $x = b_1(y)$ and $x = b_2(y)$ are given by the generalized function

$$x = \{(k-l)b_1(y) + lb_2(y)\}/k \tag{13}$$

where $k = m$, the number of gridlines in *x*-direction and *l* is an integer with $0 \le l \le k$.

The system of gridlines oriented to $y = 0$ and $y = L$ are given by the generalized function

$$y = \{(q-p)0 + pL\}/q \tag{14}$$

Where $q = n$, the number of gridlines in *y*-direction and *p* is an integer with $0 \le p \le q$.

Note that equation (13) reduces to $x = b_1(y)$ and $x = b_2(y)$ for $l = 0$ and $l = k$ respectively. Similarly equation (14) reduces to $y = 0$ and $y = L$ for $p = 0$ and $p = q$ respectively. Now by proper choice of *l, k* and *p, q* the boundary-fitted curvilinear grids can be generated.

2.4 *Coordinate Transformation*

To facilitate the numerical treatment of an irregular boundary configuration, a coordinate transformation is introduced, similar to that in Johns et al. (1985), which is based upon a new set of independent variables η, λ, y, t where

$$\eta = \frac{x - b_1(y)}{b(y)}, \quad \lambda = \frac{y}{L}, \quad b(y) = b_2(y) - b_1(y) \tag{15}$$

This mapping transforms the analysis area enclosed by $x = b_1(y), x = b_2(y), y = 0$ and $y = L$ into a rectangular domain given by $0 \le \eta \le 1, \quad 0 \le \lambda \le 1$. Also the generalized function (13) takes the form

$b\eta + b_1 = \{(k-l)b_1(y) + lb_2(y)\}/k$

which can be written as

$\eta = \frac{l(b_2 - b_1)}{bk}$. This means

$$\eta = \frac{l}{k} \tag{16}$$

The generalized function (14) takes the form
$\lambda L = \{(q-p)0 + pL\}/q$, which implies

$$\lambda = \frac{p}{q} \tag{17}$$

For $l = 0$, we have the eastern coastal boundary $\eta = 0$ or $x = b_1(y)$ and for $l = k$ we have the western open-sea boundary $\eta = 1$ or $x = b_2(y)$. Similarly, for $p = 0$, we have the southern open sea boundary $\lambda = 0$ or $y = 0$ and for $p = q$ we have the northern open-sea boundary $\lambda = 1$ or $y = L$. Thus by the proper choice of the constants k and q and the parameters l and p, a rectangular grid system can be generated in the transformed domain. Figures 2a and 2b show the physical and transformed domains and their grids.

2.5 ***Representation of Islands***

Every boundary of each island has been broken into several segments and every segment has been aligned either along (13) or along (14) so that the boundaries of every island are aligned along the boundary fitted gridlines. The representation of the island boundaries are done in such a way so that the whereabouts of them have not been lost in the transformed domain. Each of the eastern and western boundaries of an island is given by (13) and each of the southern and northern boundaries of an island is given by (14).

$l = 0$ implies $x = b_1(y)$ or $\eta = 0$ i.e. the coastal boundary and $l = k$ implies $x = b_2(y)$ or $\eta = 1$ i.e. the open boundary. Equation (13) with two different values of l, say, l_1 and l_2 with $l_1 < l_2$ will express the eastern and western boundaries of an island. Similarly equation (14) with two different values of p, say p_1 and p_2 with $p_1 < p_2$, will express the south and north boundaries of the island. Thus the transformed boundaries of an island are expressed as

$$\eta = l_1/k,\ \eta = l_2/k,\ \lambda = p_1/q, \lambda = p_2/q \tag{18}$$

2.6 ***Transformed Shallow Water Equations and Boundary Conditions***

By using the transformations (15), we have

$$\frac{\partial}{\partial x} \equiv \frac{1}{b}\frac{\partial}{\partial \eta} \tag{19}$$

$$\frac{\partial}{\partial y} \equiv -\frac{1}{b}\left(\frac{db_1}{dy} + \eta\frac{db}{dy}\right)\frac{\partial}{\partial \eta} + \frac{1}{L}\frac{\partial}{\partial \lambda} \tag{20}$$

Taking η, λ, y, t as the new independent variables and using the relations (19) and (20), the equations (4) – (6) transform to

$$\frac{\partial (bL\xi)}{\partial t} + \frac{\partial \tilde{U}}{\partial \eta} + \frac{\partial \tilde{V}}{\partial \lambda} = 0 \tag{21}$$

$$\frac{\partial \tilde{u}}{\partial t} + \frac{\partial (U\tilde{u})}{\partial \eta} + \frac{\partial (V\tilde{u})}{\partial \lambda} - f\tilde{v} = -gL(\xi + h)\frac{\partial \xi}{\partial \eta} - \frac{C_f \tilde{u}\left(u^2 + v^2\right)^{1/2}}{\xi + h} \tag{22}$$

$$\frac{\partial \tilde{v}}{\partial t} + \frac{\partial (U\tilde{v})}{\partial \eta} + \frac{\partial (V\tilde{v})}{\partial \lambda} + f\tilde{u} = -g(\xi + h)\left[b\frac{\partial \xi}{\partial \lambda} - L\left(\frac{db_1}{dy} + \eta \frac{db}{dy}\right)\frac{\partial \xi}{\partial \eta}\right] - \frac{C_f \tilde{v}\left(u^2 + v^2\right)^{1/2}}{\xi + h} \tag{23}$$

where, $U = \frac{1}{b}\left[u - \left(\frac{db_1}{dy} + \eta \frac{db}{dy}\right)v\right]$, $V = \frac{v}{L}$, $(\tilde{u}, \tilde{v}, \tilde{U}, \tilde{V}) = bL(\xi + h)(u, v, U, V)$

At $x = b_1(y)$ *i.e.* at $\eta = 0$,

$$U = \frac{1}{b}\left[u - \left(\frac{db_1}{dy} + \eta \frac{db}{dy}\right)v\right] = \frac{1}{b}\left[u - \frac{db_1}{dy}v\right] = 0.$$

At $x = b_2(y)$ *i.e.* at $\eta = 1$,

$U = \frac{1}{b}\left[u - \left(\frac{db_1}{dy} + 1 \cdot \frac{db}{dy}\right)v\right] = \frac{1}{b}\left[u - \frac{db_2}{dy}v\right]$, which can be written as $bU = u - \frac{db_2}{dy}v$.

Therefore the boundary conditions (9) – (12) reduces to

$U = 0$ at $\eta = 0$ (24)

$bU - (g/h)^{1/2}\xi = 0$ at $\eta = 1$ (25)

$VL + (g/h)^{1/2}\xi = 0$ at $\lambda = 0$ (26)

$VL - (g/h)^{1/2}\xi = 0$ at $\lambda = 1$ (27)

At each boundary of an island, the normal component of the velocity vanishes. Thus, the boundary conditions of an island are given by

$U = 0$ at $\eta = l_1 / k$ and $\eta = l_2 / k$ (28)

$V = 0$ at $\lambda = p_1 / q$ and $\lambda = p_2 / q$ (29)

3. Numerical Discretisation

The transformed shallow water equations and boundary conditions were discretised on a staggered (η, λ) grid and solved by a finite difference scheme.

We define the grid points (η_i, λ_j) in the domain by

$$\eta = \eta_i = (i-1)\Delta\eta, \qquad i = 1, 2, 3, \ldots, m \tag{30}$$

$$\lambda_j = (j-1)\Delta\lambda, \qquad j = 1, 2, 3, \ldots, n \tag{31}$$

The sequence of discrete time instants is given by

$$t_k = k\,\Delta t, \qquad k = 1, 2, 3, \ldots \tag{32}$$

The curvilinear grid system is generated through (13) and (14). In the transformed domain the corresponding rectangular grid system is generated through (16) and (17) with appropriate choices of k, q, p and l. The curvilinear boundaries and grids in the physical domain and the corresponding rectangular boundaries and grids in the computational domain are shown in Fig. 2.

The η-axis is directed towards west at an angle 15° (anticlockwise) with the latitude line and the λ-axis is directed towards north inclined at an angle 15° (anticlockwise) with the longitude line through the origin. In this model the analysis area is extended from 2° N to 14° N latitudes (incorporating the west coasts of Malaysia including Penang and Southern Thailand including Phuket) and 91° E to 100.5° E longitudes. The number of grids in η and λ - directions are respectively m = 230 and n = 319. The model area includes the source region of the Indonesian tsunami of 2004. At the ocean boundary, radiation condition, in which the tsunami wave is assumed to go out without changing its shape, is assumed. At the land boundary (coast), total reflection is assumed. The coastal boundary is fixed; that is, no run-up on the land is considered. The time step of computation is determined so as to satisfy the stability condition (Courant condition) and is set to 10 s in this computation. Following Kowalik et al. (2005), the value of the friction coefficient C_f is taken as 0.0033 throughout the model area. The depth data for the model area are collected from the Admiralty bathymetric charts.

4. Initial condition

Tsunami generation is commonly modeled by assuming that the initial sea surface displacement is formed by the permanent vertical displacement of the ocean bottom induced by an earthquake. The generation mechanism of the 26 December 2004 tsunami was mainly due a static seabed deformation caused by an abrupt slip at the India/Burma plate interface. The estimation of the extent of the earthquake rapture as well as the maximum uplift and subsidence of the seabed is given in Kowalik et. al.(2005). From the deformation contour, it is seen that the estimated uplift and subsidence zone is between 92° E to 97°E and 2°N to 10°N with a maximum uplift of 507 cm at the west and maximum subsidence of 474 cm at the east so that the uplift to subsidence is approximately from west to east. We assume that this sea surface displacement is the same as the ocean bottom displacement, due to incompressibility of the ocean. Following Kowalik et. al. (2005) the disturbance in the form of rise and fall of sea surface is assigned as the initial condition in the model with a maximum rise of 5 m to maximum fall of 4.75 m to generate the response along the western open boundary. In all other regions the initial sea surface deviations are taken as zero. Also the initial velocity components in η and λ - directions are taken as zero throughout the model area.

5. Results and Discussions

In this section, numerical results are given for the model described in the previous sections. Wave propagation from the source is computed and the water levels along the coastal belts of Phuket and Penang Islands are estimated. Every computed water level is measured with respect to the mean sea level.

Figure 3 shows the time, in minutes, for attaining +0.1 m sea level rise computed through the model. Considering the 0.1 m sea level rise as the arrival of tsunami, it is seen that after generating the initial tsunami wave at the source region, the disturbance propagates gradually towards the coast. The arrival times of initial tsunami at Phuket and Penang Island are approximately 110 min and 240 min. According to USGS report the tsunami waves reached at Phuket within two hours time after the earthquake [(http://staff.aist.go.jp/kenji.satake/Sumatra-E.html) (Tsunami travel time in hours for the entire Indian Ocean)]. The above USGS website data also confirms the fact that the tsunami waves reached Penang Island four hours after the earthquake. Hence the time of tsunami strike at the coastal regions matches well with the observations. In an earlier study (Roy et al. 2006), it is reported that the tsunami waves reached at Phuket and Penang Islands within 90 min and 230 min respectively. While the agreement of earlier study is quite good, there is a slightly better agreement in timing in the present study using boundary-fitted curvilinear grids.

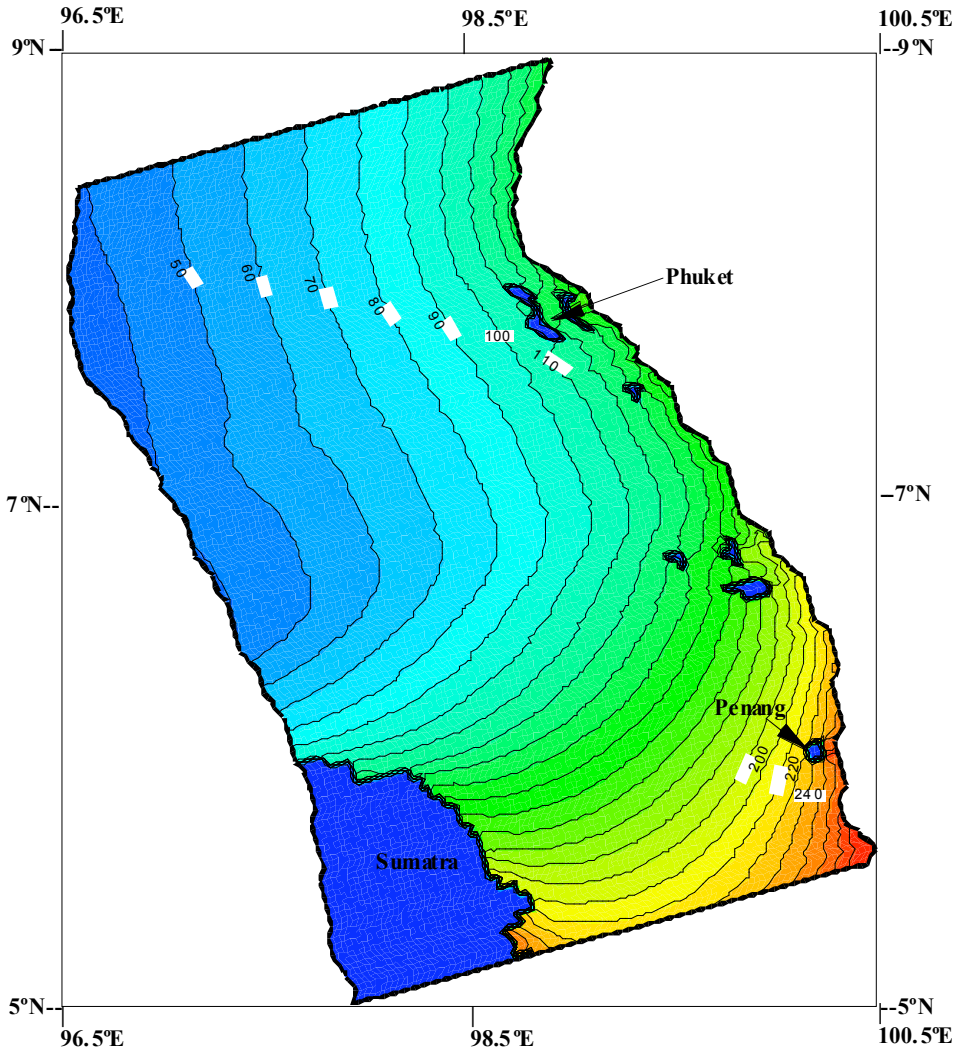

Figure 3: Tsunami propagation time in minutes towards Phuket and Penang Islands

The propagation of the tsunami towards the west coast of Peninsular Thailand and Malaysia can also be seen in Fig. 4, where the sea surface disturbance pattern is shown at four different instants of time. At 60 min after the generation of the initial tsunami wave at the source, the sea surface disturbance is found to be proceeding towards Phuket (Fig. 4a). At 110 min the tsunami has proceeded considerably towards Penang Island after flooding the Phuket region (Fig. 4b). In 180 min the disturbance propagates further towards Penang Island and finally at 240 min the tsunami surge is hitting the north and west coasts of Penang Island (Fig. 4c, d).

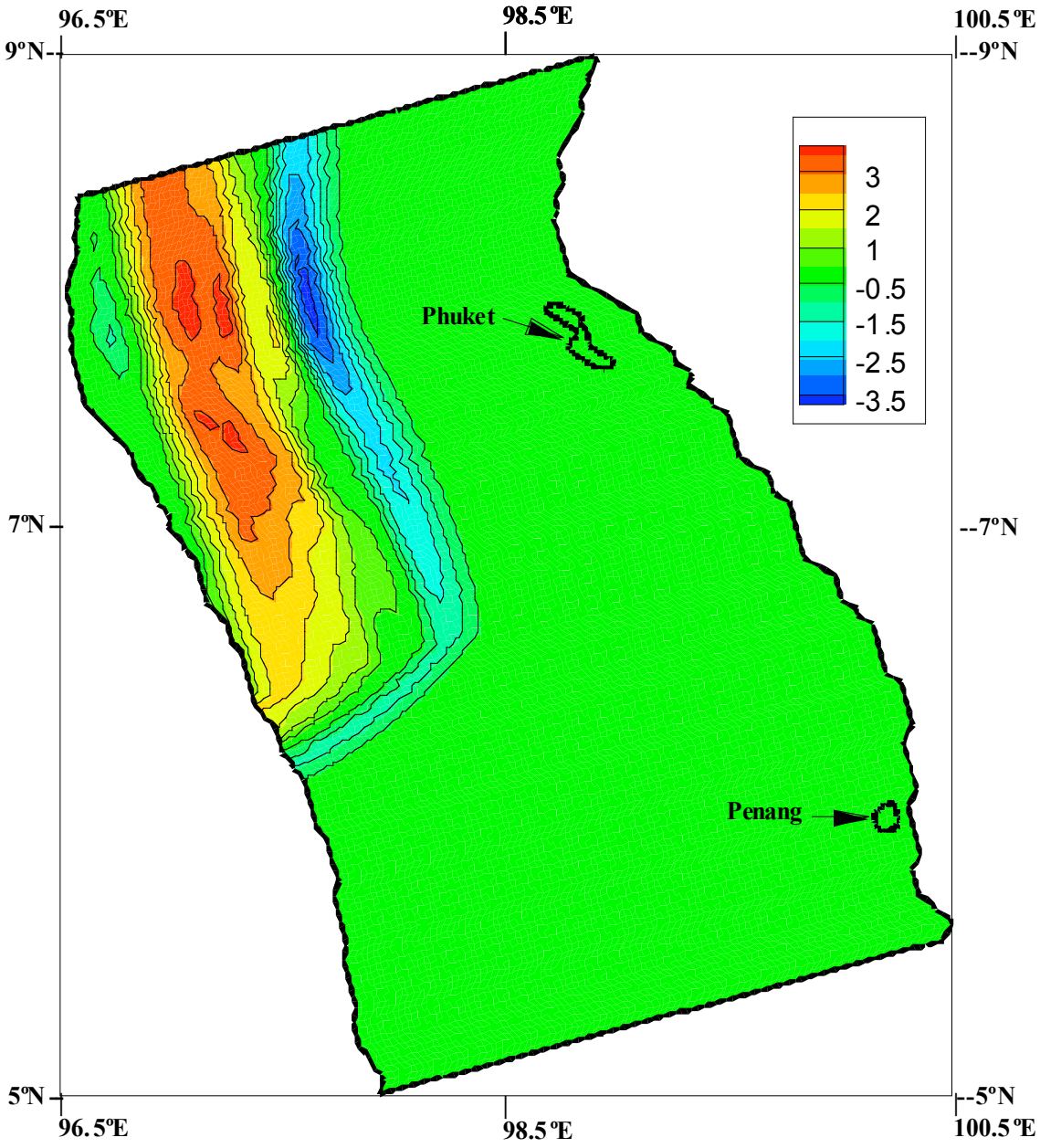

Figure 4a: Computed tsunami disturbance pattern at 60 min

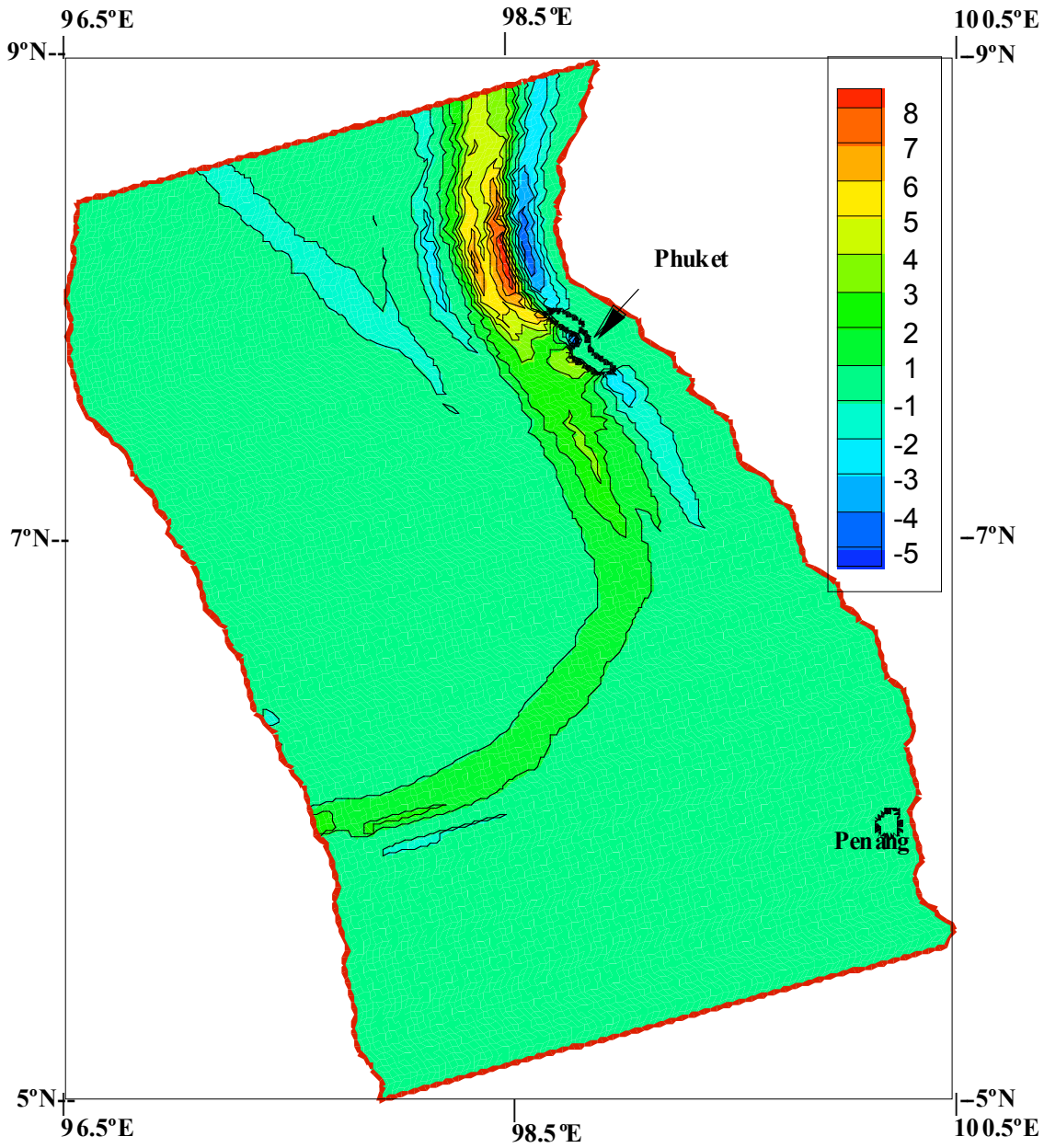

Figure 4b: Computed tsunami disturbance pattern at 110 min

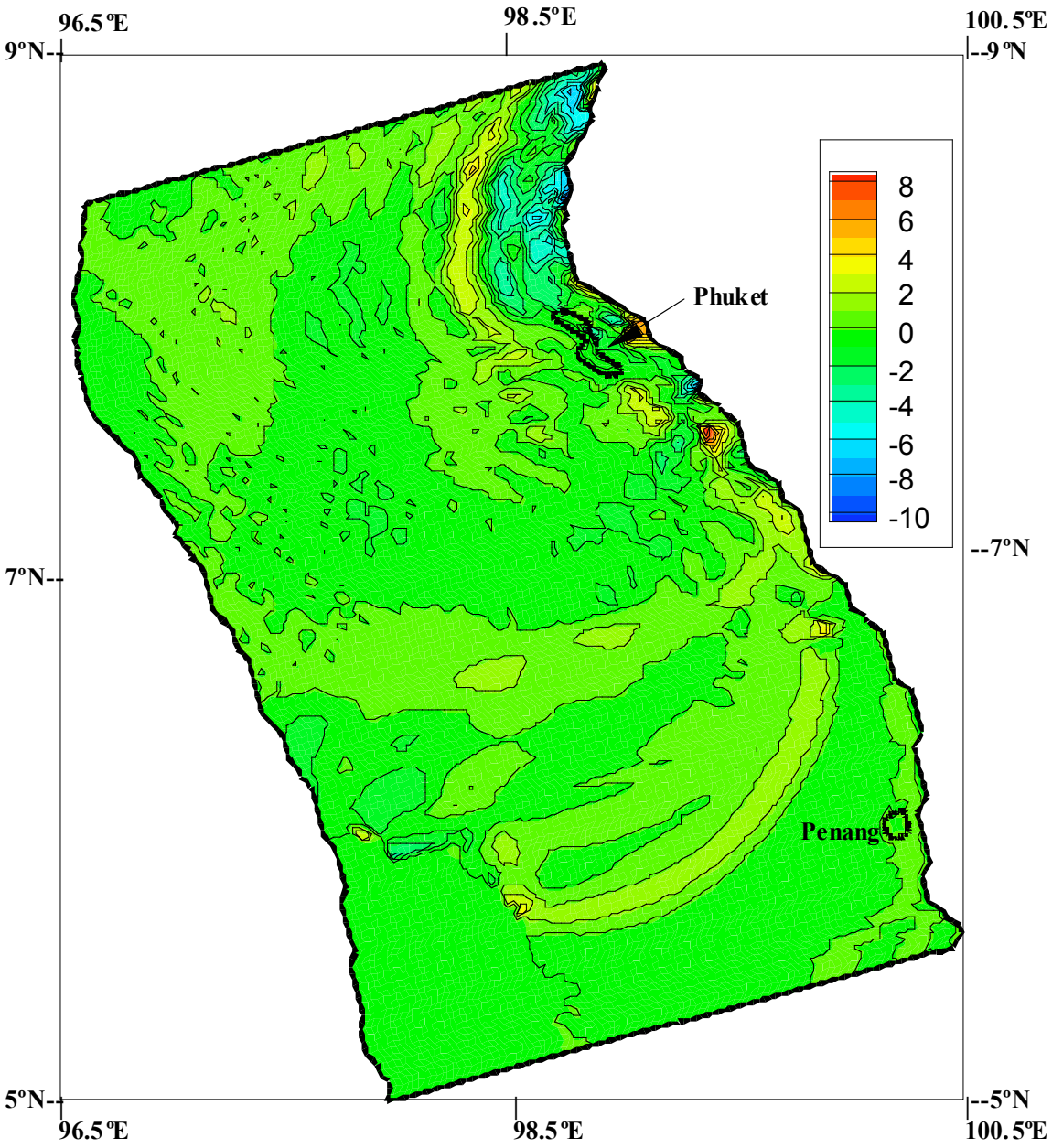

Figure 4c: Computed tsunami disturbance pattern at 180 min.

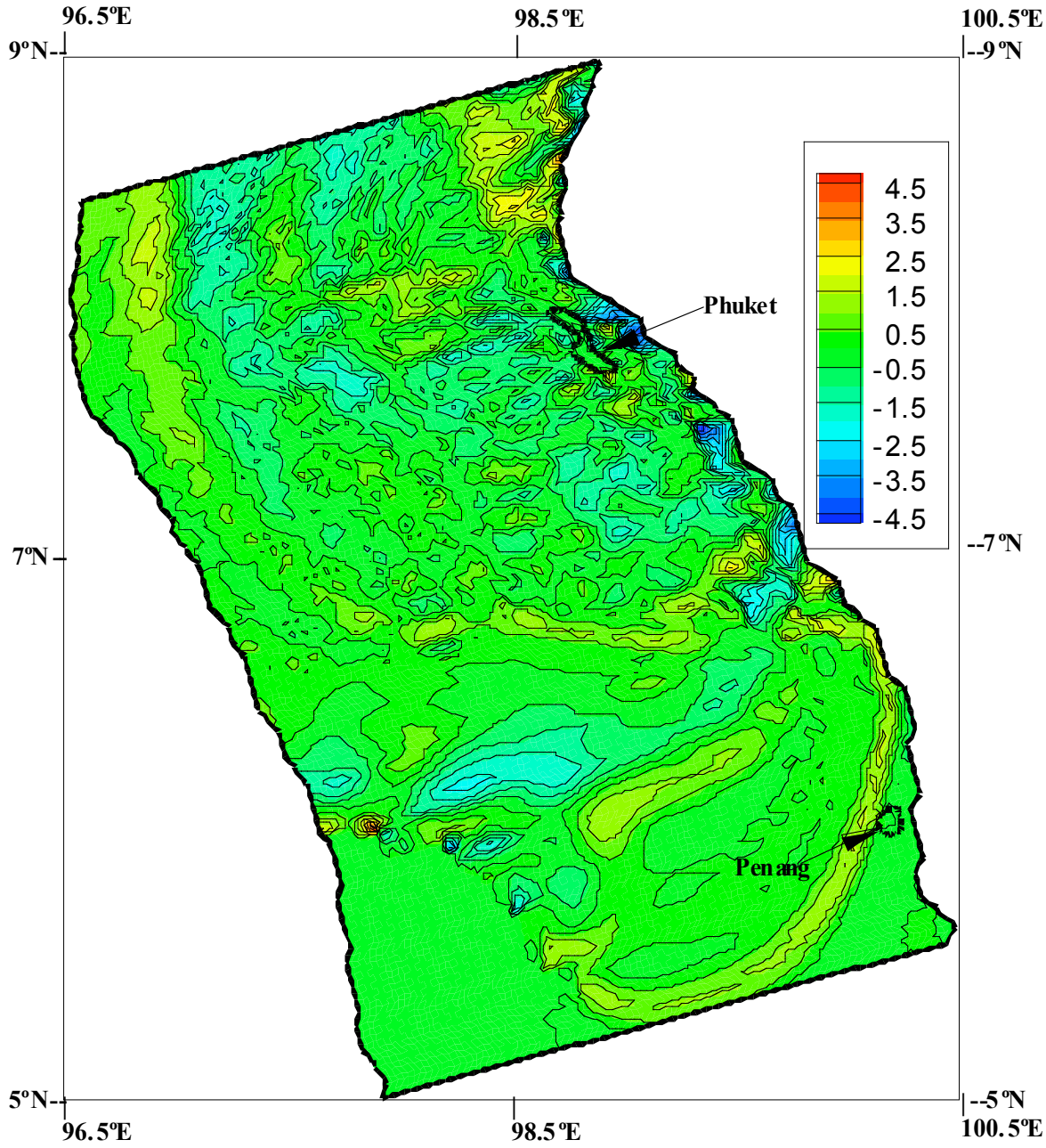

Figure 4d: Computed tsunami disturbance pattern at 240 min.

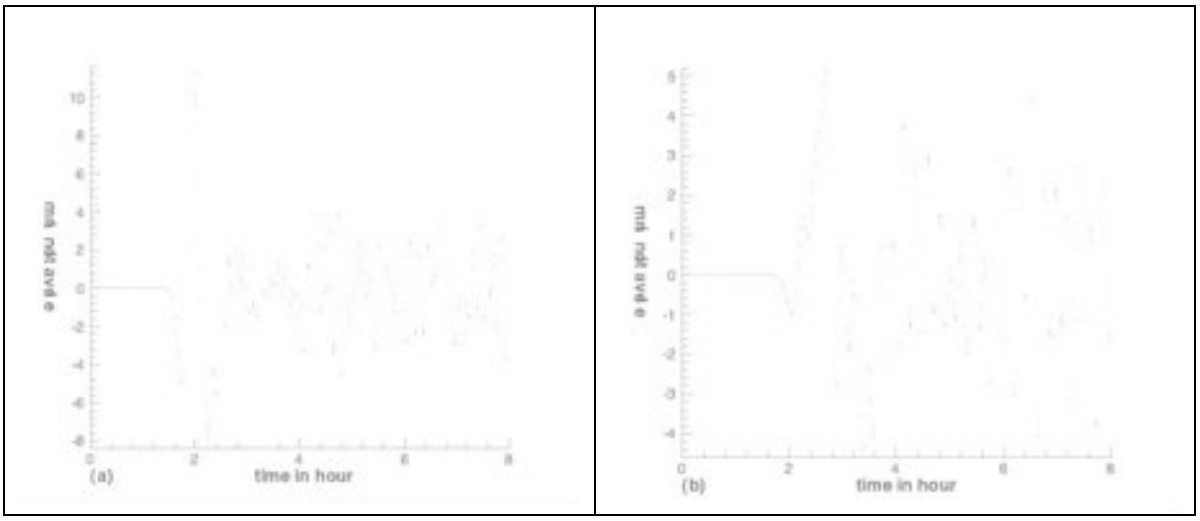

Figure 5: Time series of computed elevations at two coastal locations of Phuket Island: (a) West coast; (b) East coast

The computed water levels at different locations of the coastal belt of Phuket and Penang Island are stored at an interval of 30 seconds. Figure 5 depicts the time series of water levels at two locations of Phuket. At the west coast, the fluctuation begins with recession that reaches up to minimum level of –8.0 m before rising up; then the water level gradually increases to reach a maximum level of 11.6 m. The fluctuation then continues for several hours with low amplitude (Fig. 5a). At the east coast of Phuket also the fluctuation begins with recession reaching a minimum level of – 4.4 m. Then the water increases to a maximum level of 5.2 m before going down again; the oscillation then continues with low amplitude (Fig. 5b). Figure 6 shows the time series of water levels at two locations of Penang Island. At Batu Ferringi (north coast) the fluctuation begins with recession; the minimum and maximum levels attained are respectively – 3.4 m and 2.6 m (Fig. 6a). At the west coast the fluctuation is also oscillatory with minimum and maximum elevations of – 2.2 m and 3.2 m respectively (Fig. 6b).

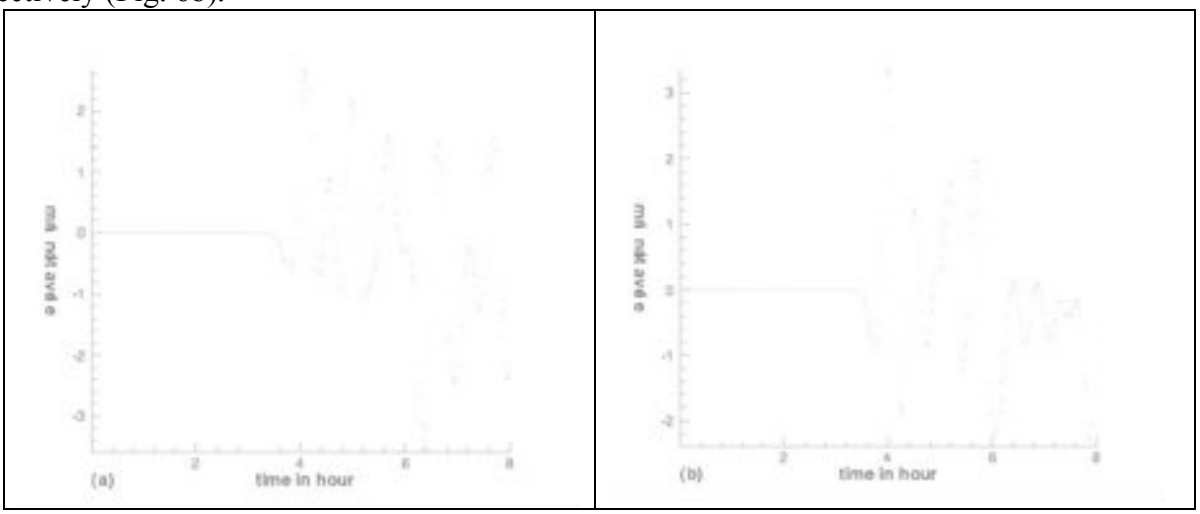

Figure 6: Time series of computed elevations at two coastal locations of Penang Island: (a) North coast; (b) West coast.

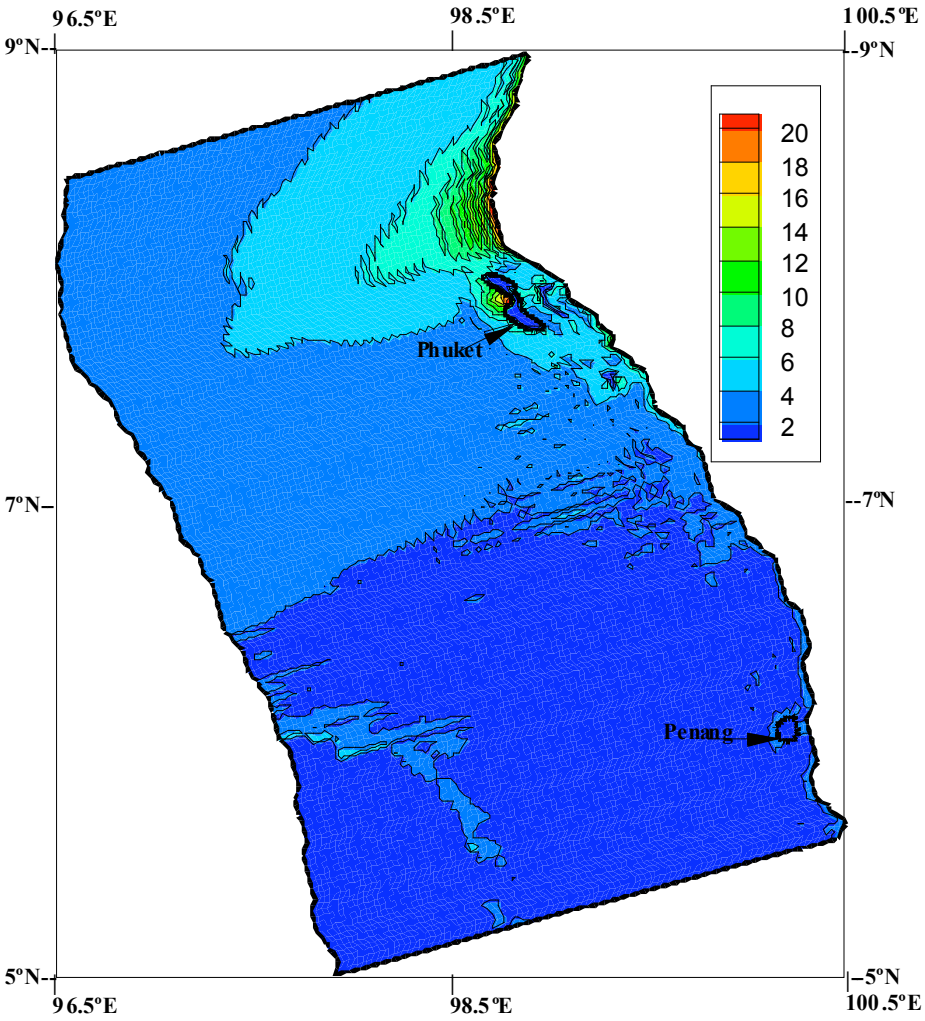

Figure 7: Contour of maximum elevation around Phuket and Penang Islands.

Figure 7 depicts the maximum water level along the west coast of Peninsular Malaysia and Thailand. It is found that the maximum water level gradually decreases in the southern direction. In the Phuket region the maximum water level ranges from 6 m to 12 m from south to north. The maximum coastal surge estimated by this model varies from 18 - 20 m in some locations located approximately 50 km north from the Phuket. We compare the computed maximum surge levels with that available in the website (www.drgeorgepc.com/Tsunami2004/Indonesia.html) and Tsuji et al. (2006). In this website address it is reported that wave height reached 7 to 11 m surrounding Phuket Island. Tsuji et al. (2006) reported that the largest tsunami height reached up to 19.6 m at Ban Thung Dap located at 50 km north from the Phuket. Thus, comparison with USGS website and study of Tsuji et al. (2006) is quite good for the Phuket region. Roy et al. (2006) reported that the computed

maximum water level at Phuket region is from 3.5 m to 7 m. So the coastal surge estimated by the present model shows better agreement with USGS than that of Roy et al. (2006).

The maximum elevation at Penang Island ranges from 2 m to 4 m along the west coast with an increasing trend towards the north. On the east coast, the measures tsunami heights show a decreasing trend towards the north. The coastal surge estimated by this model for Penang region matches reasonably well with the reported information of Roy et al. (2006).

6. Conclusions and recommendations

The results of this study indicate that boundary-fitted shallow water model is a powerful tool for simulating tsunami along a coastal belt, which is curvilinear in nature. As compared with other models, this model can make the grids fit the boundaries and can facilitated the handling of boundary conditions as well as the numerical simulation. Thus, the model has high simulation accuracy, especially in the vicinity of boundaries.

A shortcoming of the curvilinear boundary fitted representation is its inability to represent coastal and islands orographical detail. To incorporate the bending of coasts and the offshore islands with considerable accuracy in the numerical scheme, a very fine mesh numerical scheme is necessary. A nested numerical scheme (inner model with fine resolution) within the original model (outer model with high resolution) can be developed to record the fine orographical detail in the regions of principal interest. This work is ongoing and findings will be reported in our subsequent paper.

Acknowledgements

The authors acknowledge financial support from a short-term grant of University Sains Malaysia.

REFERENCES

Abbott, M.B., Damsgaard, A., Rodenhuis, G.S. 1973: System 21, 'Jupiter' A design system for two-dimensional nearly-horizontal flows, J. of Hydraulic Research, 11(1), 1 -28.

Androsov, A. A., Vol'tzinger, N. E., Liberman, Y. M. 1997: A two-dimensional tidal model of the Barents Sea. Oceanology, 37, 16-22.

Dube, S.K., Sinha, P.C., Roy, G.D. 1985: The Numerical Simulation of Storm Surge along the Bangladesh. Coast. Dyn. Atms. Oceans, 9, 121-133.

Falconer, R.A. 1980, Numerical modeling of tidal circulation in harbours, J. Waterway, Port, Coastal and Ocean Div., Proc. ASCE, 106, WW1, 31 – 48.

Heaps, N. S. 1973. A three dimensional numerical model of the Irish Sea. Geophys. J. Astorn. Soc. 35, 99 - 120.

Johnson, B.H. 1982. Numerical modeling of estuarine hydrodynamics on a boundary-fitted coordinate system in Numerical Grid Generation (Thompson, J., ed.). Elsevier, 419-436.

Johns B. Dube, S.K. Mohanti, U.C., Sinha, P.C. 1981: Numerical Simulation of surge generated by the 1977 Andhra cyclone; Quart. J. Roy. Soc. London 107, 919 – 934.

Karim, M. F., Roy, G. D., Ismail, A. I. M., and Meah, M. A. 2006, A linear Cartesian coordinate shallow water model for tsunami computation along the west coast of Thailand and Malaysia. Int. J. Ecol. & Dev., 4(S06), 1-14.

Kowalik, Z., Knight, W., Logan, T., and Whitmore. P. 2005, Numerical Modeling of the Global Tsunami: Indonesian Tsunami of 26 December 2004, Sc. of Tsunami Hazards, 23(1), 40-56.

Pararas-Carayannis, G. (2005) http://www.drgeorgepc.com/Tsunami 2004/Indonesia.html

Roy, G.D., Izani, A. M. I. 2005, An investigation of 26 December 2004 tsunami waves towards the west coast of Malaysia and Thailand using a Cartesian coordinates shallow water model, Proc. Int. Conf. Math. & Applications, Mahidol University, Thailand, 389 – 410.

Roy, G. D., Karim, M. F., Ismail, A. M.; 2006, Numerical Computation of Some Aspects of 26 December 2004 Tsunami along the West Coast of Thailand and Peninsular Malaysia Using a Cartesian Coordinate Shallow Water Model. Far East J. Appl. Math. 25(1): 57-71.

Roy, G. D., Humayun Kabir, A. B. M., Mandal, M. M., Haque, M. Z. 1999, Polar Coordinate Shallow Water storm surge model for the coast of Bangladesh, Dyn. Atms. Ocean, 29, 397-413.

Spaulding, M.L. (1984). A Vertical Averaged Circulation Model Using Boundary-fitted Coordinates. Journal of Physical Oceanography, 14, 973-982.

Tsuji, Y., Namegaya, Y., Matsumoto, H., Iwasaki, S., Kanbua, W., Sriwichai, M., Meesuk, V. 2006, The 2004 Indian tsunami in Thailand: Surveyed runup heights and tide gauge records, Earth Planets Space, 58, 223-232.